Deformation Characteristics of Granular Base Course in Flexible Pavements

SAFWAN KHEDR

ABSTRACT

The results of a triaxial test program performed on untreated granular crushed limestone base course material are presented. Triaxial tests were performed with time-variable confining pressure that varied simultaneously with the vertical dynamic loading. The test setup was designed to simulate the traffic-induced stress state on the granular base in flexible pavements. Various levels of stress state were applied to samples of different moisture contents and relative densities. The analysis of permanent deformation results revealed that a power relationship existed between the rate of permanent strain accumulation and the applied number of loading cycles. Further, the exponential parameter m in the relationship was found to vary over a limited range for all tested samples. The intersection parameter A, which expressed the rutting susceptibility of the material, was found to be most sensitive to stress state and resilient modulus. Parameter A was expressed in a power relationship to the octahedral stress ratio and the resilient modulus. The resilient modulus variation was investigated and found to depend mainly on the stress state. For deviator stress higher than 10 psi, the resilient modulus had a power relationship with the first stress invariant. Furthermore, the exponent of that relationship is linearly interrelated with the logarithm of the intersection coefficient of the same relationship.

A granular base course has a significant effect on the resilient deflection as well as on the residual deformation of a flexible pavement system (1). The degree of significance depends on pavement design structure and environmental conditions. One example is incorporating a free-draining base course to facilitate proper drainage for the pavement. A free-draining granular base, which contains a very low percentage of fines, may contribute to both resilient and residual deformation of the pavement.

The response of granular material under dynamic loading that simulates traffic is different from that under static loads. Therefore it should be tested under dynamic stresses of a magnitude expected in a pavement structure in order to characterize the material for the evaluation of pavement response under traffic. This has been recognized by researchers since 1958 (2). Several investigators have reported experimental results obtained from such tests (3-5). In these and other studies, efforts were directed toward resilient or residual characterization, or both, of granular material.

Barksdale (6) pioneered comprehensive experimental research to investigate the plastic deformation of a variety of granular materials. Ten different materials and blends were tested under constant confining pressure and uniaxial dynamic stress of triangular loading function. In his study Barksdale presented many conclusions that explained various points about deformations of granular materials and served as the basis for further refining research in the field. Some of these conclusions were:

1. Plastic strain accumulated approximately logarithmically with the number of load applications.
2. Threshold deviator dynamic stress existed beyond which the rate of strain accumulation tended to increase with the number of load repetitions.
3. Plastic strain was almost proportional to deviator dynamic stress at static confining pressure for small values of deviator stress.
4. Plastic and elastic strains were strongly dependent on confining pressure, undergoing a significant decrease with increasing confining pressure.
5. The plastic stress-strain curves exhibited a typical nonlinear response similar to those in monotonic stress conditions. A hyperbolic expression was suggested to describe the curves:

$$\epsilon_a = [(\sigma_1 - \sigma_3)/(k\sigma_3^n)]/\left(1 - \left\{[(\sigma_1 - \sigma_3)R_f(1 - \sin\phi)] \div (2c\cos\phi + \sigma_3\sin\phi)\right\}\right) \quad (1)$$

where

ϵ_a = axial strain,
$k\sigma_3^n$ = relationship defining the initial tangent modulus as a function of the confining pressure (σ_3) (k and n are constants),
c = cohesion,
ϕ = angle of internal friction, and
R_f = a constant relating compressive strength to an asymptotic stress difference.

Equation 1 was suggested at a particular number of loading repetitions. However, in applying Equation 1 in a particular estimation of rut depth with pavement performance life, an extensive testing program would be needed to calculate the parameters in the equation at various numbers of load repetitions.

Allen (4) conducted a series of experiments on nine samples of granular material in which both time-variable and constant confining pressures were applied. Although his study was not intended to investigate permanent deformation, he made the general comments that plastic strain decreased with increasing material density and that crushed stone speci-

mens experienced less plastic strain than the gravel specimen, which suffered the most plastic strain under the same stresses.

A laboratory dynamic triaxial test was conducted by the National Crushed Stone Association (NCSA) (7) to study the characteristics of plastic deformation of graded aggregates. Kalcheff (7) reported that the plastic strains were greatly dependent on the degree of consolidation for the same gradation, the amount and type of fines in the gradation, the stress sequence and magnitude, and the moisture content for some types of fines. In keeping with Barksdale's observation, Kalcheff noted that plastic strain accumulated approximately logarithmically with the number of load repetitions.

In the flexible pavement model VESYS II (8), it was suggested that the permanent deformation in flexible pavement layers be represented in the format

$$\epsilon_a = IN^S \tag{2a}$$

$$\epsilon_p = ISN^{S-1} \tag{2b}$$

$$F(N) = MN^{-\alpha} \tag{2c}$$

where

ϵ_a = permanent strain at N cycles,
I = intercept coefficient,
S = slope coefficient,
ϵ_p = permanent strain due to the Nth loading,
F(N) = fraction of total strain due to the Nth loading that is permanent,
M = IS/ϵ_r,
α = 1 - S, and
ϵ_r = resilient strain.

The system incorporated Equations 2a, 2b, and 2c in a predictive technique that used the similarity between the permanent strain cumulative curve and the static creep curve.

Numerous research efforts in the 1970s were devoted to the study of resilient deformations in granular materials as an element in flexible pavements (4,5,7,9,10). Hicks (5) and Allen (4) have reached, in separate efforts, similar conclusions about the resilient characteristics of granular materials. Some of these conclusions were

1. The resilient response of granular materials was independent of the stress pulse duration (for a duration time range of 0.1 to 0.2 sec).
2. The resilient response of granular material was significantly affected by the applied stress history. However, the response was fairly steady and stable after approximately 100 cycles of constant stress-amplitude dynamic loading.
3. Higher density material exhibited higher resilient modulus.
4. The stress level and condition were the factors with most influence on the resilient properties of granular materials. They found that either

$$M_R = k_1 \theta^{k_2} \tag{3}$$

or

$$M_R = k_3 \sigma_3^{k_4} \tag{4}$$

where

M_R = resilient modulus,
k_1, k_2, k_3, k_4 = regression constants,
σ_3 = confining pressure, and
θ = sum of principal stresses = $\sigma_1 + 2\sigma_3$

would represent the modulus-stress state relationship. Allen, however, found that Equation 3 had a higher correlation coefficient in the regression analysis.

5. Allen observed that the constant confining pressure (CCP) tests generally overestimated the resilient Poisson's ratio compared with the results of the dynamic confining pressure (DCP) tests. He also observed that the resilient modulus calculated from CCP tests exceeded that computed from the DCP test. However, this conclusion was not verified for all nine samples tested. Therefore he concluded that the continued use of the CCP triaxial test as a means of characterizing granular materials was justified.

The elastic layered solution has been frequently used as a technique for analyzing a flexible pavement system that contains untreated granular base or subbase, or both. However, because of the unrealistic tensile radial stresses calculated in these granular layers, and also because of the unrealistically low radial pressures calculated when using elastoplastic theory in the finite element method, it can be seen that no model has been established that would describe and account for the behavior of such material as part of a flexible pavement system under real traffic loading (11). All models in use characterize the granular layer as a continuum. It should instead be investigated as an assembly of oriented particles. The granular material can resist a certain amount of radial tensile stresses through the interparticle friction forces that are proportional to the normal stresses at the particles' interfaces. The development of these frictional forces will increase the material's tendency to slip. Therefore passive pressure due to adjacent overburden will be mobilized and, consequently, the confining pressure will increase, causing higher strength (i.e., higher modulus) (11). Because of the cohesionless nature of the untreated granular material, it should be tested under confinement pressure. Except for a few studies (4,10), the confining pressure was kept constant during the dynamic deviator loading in previous research efforts. Such a stress arrangement (CCP) has the following disadvantages:

1. It does not simulate the in situ condition in which lateral pressure changes simultaneously with vertical pressure as a function of time (12).
2. The role of the confining pressure in that stress arrangement is limited to conditioning stress and is not a direct reaction to vertical wheel loading.
3. In triaxial testing, there are two types of procedure:
   - Preconsolidate the sample under confining pressure before applying the dynamic vertical load, thus neglecting the effect of confining pressure on permanent deformation, and
   - Apply dynamic vertical loading simultaneously with the constant confining pressure (σ_3) and thus overestimate the effect of σ_3.
4. In a triaxial cell, the confining pressure is applied on the sample in all directions, which means inducing unrealistic static overburden pressure in the vertical direction.

There has been no report of a complete constitutive equation that would describe permanent deformation in untreated granular material during pavement life. The residual characteristics of granular material have not been investigated in experimentation that involved applying dynamic confining pressure that varied simultaneously with the axial pressure on a time scale to avoid the disadvantages previously mentioned.

The objectives of this study were to investigate the deformation mechanism of untreated granular material in an experimental program that involved applying stress conditions compatible with those expected in flexible pavements. Analysis of the experimental results should lead to the development of a constitutive equation to describe the dynamic creep of the material. Such a constitutive equation would be used in schemes for predicting rutting of flexible pavements.

EXPERIMENTAL PROGRAM

A crushed limestone aggregate obtained from Franklin County, Ohio, with a maximum size of 3/4 in. and limestone fines, was subjected to a dynamic testing program. Figure 1 shows the material gradation used. The fines in the aggregate had a liquid limit of 15 percent and nonplastic properties. The specific gravities measured were 2.57 and 2.64 for the coarse and fine portions, respectively. The compaction curves for the aggregate used are shown in Figure 2.

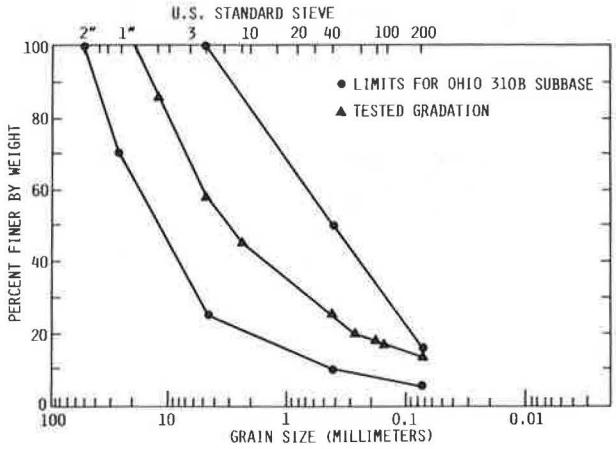

FIGURE 1 Aggregate gradation and gradation bands for Ohio 310B subbase.

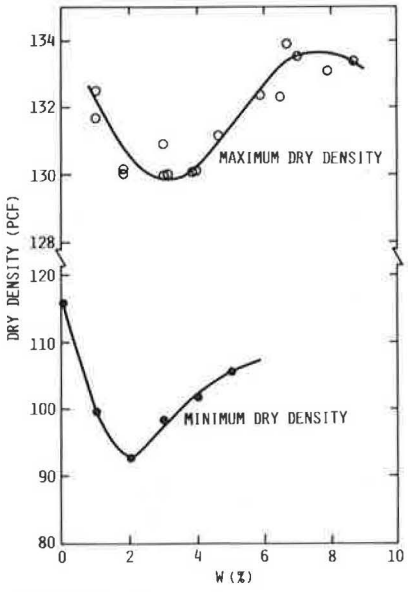

FIGURE 2 Compaction curves for tested aggregates.

Standard compaction procedure, employing the modified compaction energy, was used in determining the maximum dry density curve. The minimum dry density test was run in accordance with AASHTO T19-70. The samples involved in the testing program were 4 in. in diameter and 7.5 in. in height, compacted at 0, 4, or 6 percent water contents to approximately constant dry density of 130± pcf.

The dynamic testing involved applying simultaneous time-variable confining and deviator stresses on the aggregate samples. The tests were carried out in a triaxial cell. Figure 3 shows a schematic of the cell setup. The stresses were applied using two electronically connected material testing systems (MTSs) as shown in Figure 4. The first applied variable confining pressure with stroke control through a hydraulic setup and an oil-water interface. The second applied the required deviator stress with load control synchronized with the confining pressure. A haver-sine loading function was applied in both the vertical and the horizontal direction. The load frequency was one cycle per second with load duration of 0.125 sec. However, the cycle duration was somewhat longer for the lateral pressure because of the pressure transfer mechanism from the MTS to the triaxial cell. The static components of the ver-

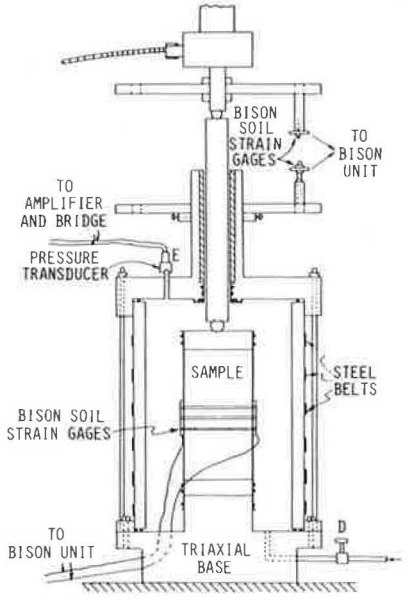

FIGURE 3 Triaxial testing arrangement.

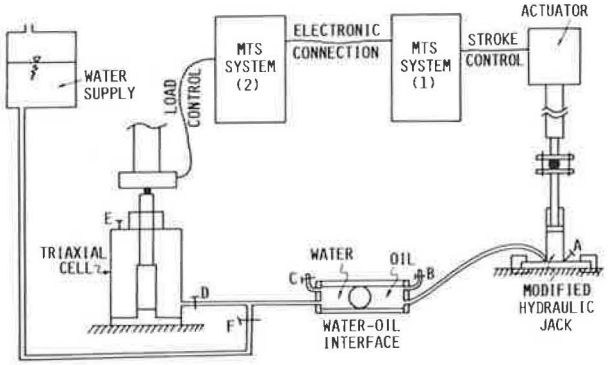

FIGURE 4 Base course testing arrangement.

TABLE 1 Physical and Ultimate Properties of Aggregate Samples

Sample No.	W (%)	γ_d (pcf)	γ_r (relative density)	Height (in.)	Static Modulus (psi)	ϕ^o
11	7.6	132.0	0.95	8.2		
21	4.6	130.0	0.92	6.75		
31	4.0	130.0	0.95	7.28	10,935	53.4
41	4.04	130.0	0.95	7.28		55.6
51	4.0	130.0	0.95	7.28	28,134	51.6
61	3.93	130.1	0.96	7.28	10,900	54.7
62	3.93	130.1	0.96	7.28	10,900	54.7
71	4.03	130.0	0.95	7.28	31,936	57.4
81	3.95	130.1	0.96	7.28	34,959	51.1
91	5.96	130.1	0.87	7.28	24,981	64.3
101	6.00	130.0	0.87	7.28	28,457	57.8
111	5.90	130.1	0.87	7.28	22,420	59.5
121	7.00	128.8	0.82	7.28	21,656	59.0
131	4.19	132.3	1.03	7.28	23,695	63.4
141	5.9	130.1	0.87	7.28	16,388	64.4
142	5.9	130.1	0.87	7.28	16,388	64.4
151	0	131.1	0.92	6.94	10,840	54.4
152	0	131.1	0.92	6.94	10,840	54.4
161	0	130.0	0.85	7.75	9,390	52.4
171	0	130.0	0.85	7.50	20,638	53.8
172	0	130.0	0.85	7.50	20,638	53.8
181	0	130.9	0.91	7.45	13,196	49.0
182	0	130.9	0.91	7.45	13,196	49.0
191	0	130.0	0.85	7.50	17,618	56.0
192	0	130.0	0.85	7.50	17,618	56.0
201	0	130.0	0.85	7.50	22,921	54.8
211	0	130.0	0.85	7.50	16,970	56.3
213	0	130.0	0.85	7.50	16,970	56.3
221	4.12	129.9	0.94	7.50	21,018	55.4
222	4.12	129.9	0.94	7.50	21,018	55.4
231	3.86	130.2	0.97	7.50	20,619	61.7
232	3.86	130.2	0.97	7.50	20,619	61.7
233	3.86	130.2	0.97	7.50	20,619	61.7
241	3.73	130.3	0.98	7.50	26,850	55.5
242	3.73	130.3	0.98	7.50	26,850	55.5

tical and confining pressures were continuously maintained throughout the test.

The dynamic tests were performed at dynamic deviator stress levels of 0, 5, 10, and 20 psi with dynamic confining pressures of 5, 10, and 15 psi applied to each group of samples having a specific water content.

The permanent and elastic deformations were monitored during every test for at least 4,000 load repetitions. All deformations were recorded using Bison soil strain gauge coils (1- and 2-in. diameters) mounted on a Plexiglas measuring assembly.

ANALYSIS OF RESULTS

Residual Deformation

Table 1 gives the physical and ultimate properties of the 24 tested samples. Table 2 gives the stress state at which each sample was tested for dynamic creep as well as its mechanical properties. Figure 5 shows two typical examples of dynamic creep results expressed in the form log ($\epsilon p/N$) versus log (N), where ϵp is the permanent strain after N load repetitions. Linear statistical regression of these results indicated the following equation:

$$\epsilon p/N = AN^{-m} \quad (5)$$

where m is material parameter and A is material and stress-state parameter.

Equation 5 was found to be applicable to all tested samples with correlation coefficients quite close to unity (correlation coefficients ranged from

TABLE 2 Stress State and Mechanical Properties of Aggregate Samples

Sample No.	Lateral Pressure (psi)		Deviatoric Pressure (psi)		Octahedral Stress (psi)		Poisson's Ratio υ	M_R (psi)	A ($\times 10^{-4}$)	m
	Static	Dynamic	Static	Dynamic	Normal σ_o	τ_o Shear				
11	10.0	0	0.96	21.0			0.45	44,000	2.597	0.688
21	1.33	8.25	2.87	18.10	14.28	8.85	0.45	21,300	5.349	0.817
31	1.08	4.10	2.46	10.78	7.69	5.08	0.473	20,200	5.146	0.903
41	4.94	0.0	1.69	24.30			0.45	30,600	8.448	0.899
51	4.84	0.0	1.67	21.42			0.44	36,400	8.05	0.908
61	1.73	4.07	1.35	1.16	4.46	0.55	0.5	13,000	0.1395	0.608
62	2.12	4.60	2.11	20.54	11.45	9.68	0.5	28,300	6.632	0.900
71	2.00	8.07	2.60	10.33	11.51	4.87	0.374	30,700	2.188	0.838
81	1.90	11.76	3.33	19.95	18.41	9.41	0.337	38,500	2.664	0.831
91	1.13	4.28	2.25	20.30	11.05	9.57	0.46	25,300	5.483	0.812
101	2.06	14.81	3.40	18.84	21.09	8.88	0.406	35,100	0.5938	0.725
111	1.88	10.30	2.68	19.96	16.95	9.41	0.409	34,200	3.716	0.827
121	1.96	10.02	2.48	11.20	13.75	5.28	0.528	24,500	4.666	0.859
131	1.08	5.11	2.38	11.02	8.78	5.19	0.55	14,800	4.521	0.864
141	0.99	5.08	2.63	0	5.08	0	0.453	45,200	0.08049	0.559
142	1.03	4.85	2.69	4.71	6.42	2.22	0.453	20,500	3.984	0.909
151	0.95	5.29	2.55	0	5.29	0	0.54	6,800	0.6455	0.743
152	1.00	5.03	2.86	4.83	6.64	2.28	0.34	9,890	1.990	0.765
161	1.06	5.00	2.26	10.95	8.65	5.16	0.716	17,100	8.367	0.767
171	1.95	14.00	2.68	0	14.00	0	0.445	35,000	0.4432	0.806
172	2.07	15.10	2.66	18.48	21.26	8.71	0.445	29,600	3.368	0.814
181	1.80	10.44	2.25	0	10.44	0	0.387	45,000	6.435	0.902
182	2.02	9.71	2.24	9.50	12.88	4.48	0.387	30,300	3.555	0.743
191	0.95	5.00	2.32	0	5.00	0	0.80	7,260	6.278	0.705
192	1.06	5.13	2.26	20.17	11.85	9.51	0.80	17,800	13.756	0.746
201	2.03	10.20	2.12	0	10.20	0	0.287	79,940	0.4303	0.861
202	2.04	10.80	2.07	18.66	17.02	8.80	0.287	34,500	4.277	0.777
211	0.89	5.10	2.29	0	5.10	0	0.522	1,550	4.414	0.903
213	1.01	5.16	2.27	19.46	11.65	9.17	0.56	27,000	37.663	0.873
221	1.95	10.15	2.14	0	10.15	0	0.442	29,400	1.759	0.875
222	2.13	10.12	2.56	9.55	13.30	4.50	0.442	33,000	0.5702	0.741
231	0.30	12.35	2.46	0	12.35	0	0.59	23,500	0.4911	0.671
232	1.00	5.21	2.29	4.38	6.67	2.07	0.59	24,300	0.2192	0.725
233	1.08	5.13	2.27	19.78	11.72	9.32	0.59	34,100	2.488	0.800
241	1.98	10.40	2.86	0	10.40	0	0.452	50,000	1.133	0.822
242	2.12	10.21	2.79	8.96	13.20	4.22	0.452	30,500	0.3279	0.699

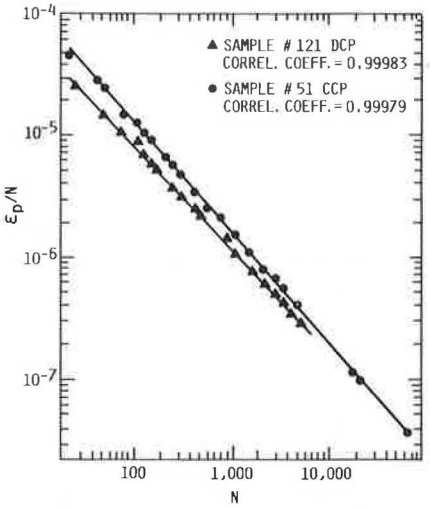

FIGURE 5 Rate of permanent strain accumulation versus number of load repetitions.

0.93 to 1.0). It should be pointed out that the results shown in Figure 5 are for Sample 121, which was tested under dynamic confining pressure (DCP), and for Sample 51, which was tested under constant confining pressure (CCP). The indicated high values of the correlation coefficients and the extremely high values of the statistic F* for the test results strongly suggest that Equation 5 accurately represents dynamic creep for granular material. However, a closer look at the regression residuals suggested that the data points on the log ($\varepsilon p/N$) versus log (N) graph tended to form a very flat convex curve that could be approximated by a straight line. A schematic (Figure 6) magnifies this trend. Nevertheless, this observation does not reduce the significance of Equation 5 accurately describing the test results. Data obtained by Chou (11) and Barksdale

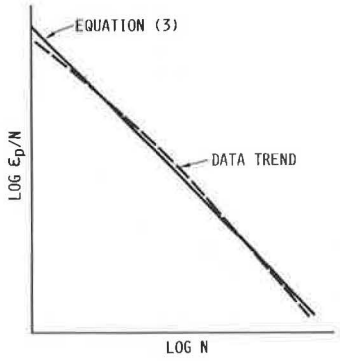

FIGURE 6 Data trend and model representation.

(6) were analyzed and found to be consistent with the same conclusion. Equation 5 verified the VESYS (8) suggestion presented in Equation 2.

In general, permanent deformation was found to increase with increasing deviator stress and decreasing confining pressure, resilient modulus, water content, static initial modulus, angle of internal friction, and relative density within the ranges considered in this study. Resilient Poisson's ratio had no apparent effect on permanent deformation.

Similar trends were observed for samples tested under zero deviator stress, defined in this paper as dynamic consolidation, except that higher dynamic confining pressure resulted in more sample consolidation. Permanent deformation cumulation was observed even for those samples the resilient Poisson's ratios of which were larger than 0.5. The dynamic consolidation followed Equation 5 as well. However, the mechanism of dynamic creep, which is mainly due to shear straining, was different from that of dynamic consolidation, which was attributed to volumetric changes. Because dynamic consolidation was of no practical significance to pavement performance, it was not investigated any further.

From Equation 5, a complete evaluation of parameters m and A should be sufficient to characterize the residual behavior of the granular material. Table 2 gives the values of m and A for each sample. They were calculated using linear regression analysis of test data. Samples 11, 41, and 51, which were tested under CCP and were not included in the analysis, are discussed in the following sections.

Parameter m in Equation 5 is the slope of the linear relationship between log ($\varepsilon p/N$) and log (N). It was found to vary within the general range of 0.7 to 0.9 (Figure 7). The overall average value of m is 0.804 with a standard deviation of 0.067.

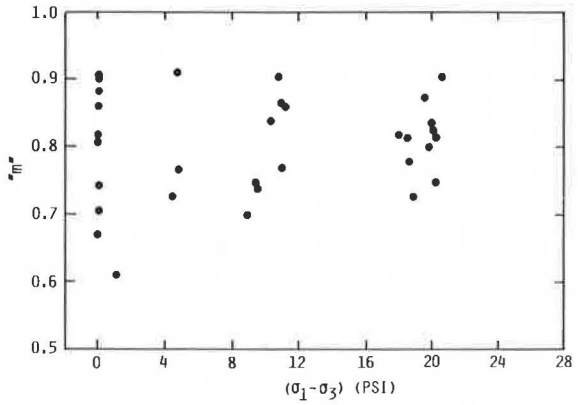

FIGURE 7 Parameter m versus deviator stress.

Multiple regression analysis of m versus resilient modulus (M_R), deviator stress ($\sigma_1 - \sigma_3$), confining pressure (σ_3), octahedral shear [$\tau_o = (2^{1/2})(\sigma_1 - \sigma_3)/3$], octahedral normal [$\sigma_o = (\sigma_1 + 2\sigma_3)/3$], water content (w), relative density (γ_r), and angle of internal friction (ϕ) revealed that m did not show a particular correlation with any of these variables. No specific trend was observed for m variation.

Figure 7 shows m variation with the applied deviator stress ($\sigma_1 - \sigma_3$). It can be seen from the figure that parameter m varied within a relatively narrow range. Therefore it could be considered constant for practical design purposes. Figure 8 shows that the confidence level of the actual mean of parameter m would lie within the shaded zone, assuming a normal distribution variation for the obtained m values.

Parameter A can be defined as the residual strain after the first load cycle is applied on the sample. Although the consideration of m as a constant is not

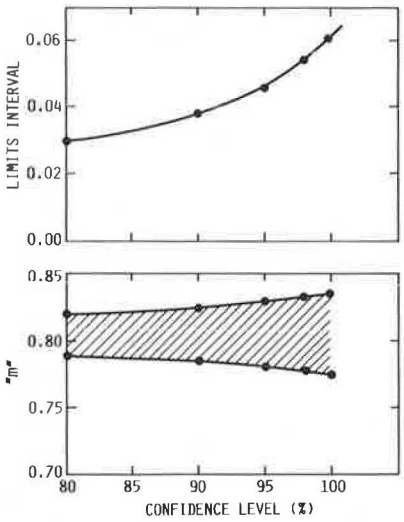

FIGURE 8 Predicted statistical range for parameter m.

strictly justified, useful information relative to the dependency of residual strains on various independent parameters may be gained by considering m a constant. In such a case, parameter A should reflect the residual behavior of the granular material (Equation 5). Statistical analysis of the test results revealed that parameters A and m were not interrelated.

Stepwise regression analysis in the power form was conducted between A and all physical and mechanical variables considered in the analysis of m variation. Only the data set with $(\sigma_1 - \sigma_3) > 0$ (i.e., dynamic creep) was considered in the analysis. The correlation array is given in Table 3. In general, parameter A had a positive correlation with $(\sigma_1 - \sigma_3)$, τ_o, σ_o, principal stress ratio $[R_p = (\sigma_1 - \sigma_3)/\sigma_3]$, and octahedral stress ratio $(R_o = \tau_o/\sigma_o)$; it had negative correlation with w, γ_r, initial static modulus (E_s), M_R, ϕ, and σ_3. It appeared to be highly dependent on either principal or octahedral stress ratio.

TABLE 3 Correlation Coefficients for Factors Affecting Parameter A and Resilient Modulus M_R

Factor	A	M_R
$(\sigma_1 - \sigma_3)$	0.637	0.552
τ_o	0.637	0.553
σ_3	-0.149	0.648
σ_o	0.241	0.731
$(\sigma_1 - \sigma_3)/\sigma_3$	0.777	0.080
τ_o/σ_o	0.798	0.130
M_R	-0.215	1.000
E_s	-0.198	0.627
tan ϕ	-0.049	0.051
w	-0.274	0.250
γ_r	-0.414	0.096

Note: All variables except w expressed in logarithm form.

Several forms of multiple regression were applied to the test results. The following expressions are examples of such forms:

$$A = c_1(\sigma_1 - \sigma_3)^{c2}(\sigma_3)^{c3} \quad (6)$$

$$A = c_4(\sigma_1 - \sigma_3)^{c5}(\sigma_3)^{c6}(M_R)^{c7} \quad (7)$$

$$A = c_8(\sigma_1 - \sigma_3)^{c9}(\sigma_3)^{c10}(M_R)^{c11}\exp(c_{12}w) \quad (8)$$

$$A = c_{13}(R_p)^{c14}(M_R)^{c15} \quad (9)$$

$$A = c_{16}(R_p)^{c17}(M_R)^{c18}\exp(c_{19}w) \quad (10)$$

where c_i are regression constants. The analysis of these regression models was done in three phases incorporating principal stresses as shown in Expressions 6-10, incorporating octahedral stresses instead of principal stresses, and finally incorporating the relative density instead of the water content. It was found that including either the relative density or the water content in the analysis would yield essentially the same results. That is, the third phase did not significantly affect the analysis.

The results of the first two phases are given in Table 4. Comparison of the correlation coefficient and the statistic F* of the different models revealed the significance of various variables for parameter A. Incorporating the octahedral stresses appeared to improve the correlation. Regression Expression 9 would then become

TABLE 4 Results of Multiple Regression Analysis of Parameter A

Model	Correlation Coefficient	F*	F
Phase 1—Incorporating Principal Stresses			
6	0.777	13.72	3.57
7	0.836	13.10	3.21
8	0.857	11.02	3.02
9	0.800	15.99	3.57
10	0.844	14.00	3.21
Phase 2—Incorporating Octahedral Stresses			
6	0.801	16.15	3.57
7	0.844	14.06	3.21
8	0.867	12.14	3.02
9	0.830	20.00	3.57
10	0.865	16.81	3.21

$$A = s_1(R_o)^{s2}(M_R)^{s3} \quad (11)$$

where s_1, s_2, and s_3 are regression constants. The values of these constants for the data presented are 0.0358, 2.135, and -0.304, respectively. Equation 11 was suggested to describe the variation of parameter A in a less-complicated form. Figure 9 shows the relationship of A versus R_o for all tested samples. It was not practically possible to control sample preparation and stress state of the dynamic test in order to produce controlled values of resilient modulus. The results shown in Figure 9 were divided into two groups that have values of resilient modulus below and above 25,000 psi, respectively.

Substituting Equation 11 into Equation 5 results in

$$\epsilon p/N = s_1(R_o)^{s2}(M_R)^{s3}N^{-m} \quad (12)$$

Equation 12 is the constitutive equation that describes the permanent strain of granular material as a function of its resilient modulus, which reflects material strength, stress state, and number of loading cycles. It can be used to predict permanent de-

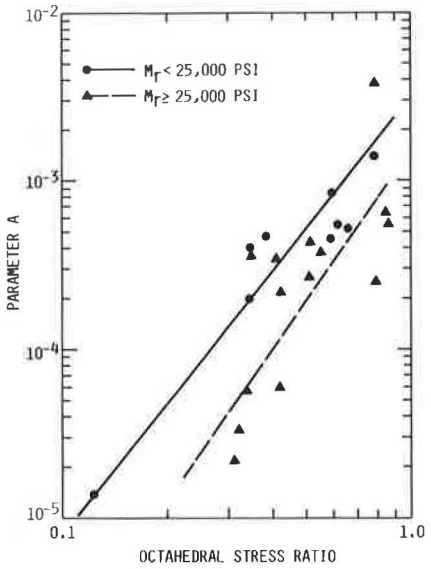

FIGURE 9 Parameter A versus octahedral stress ratio.

formation in an untreated base course along with pavement life.

Resilient Deformation

Figure 10 shows typical results of the resilient modulus versus number of loading cycles (N). The granular material reached a stable condition after 100 cycles beyond which the modulus did not vary significantly.

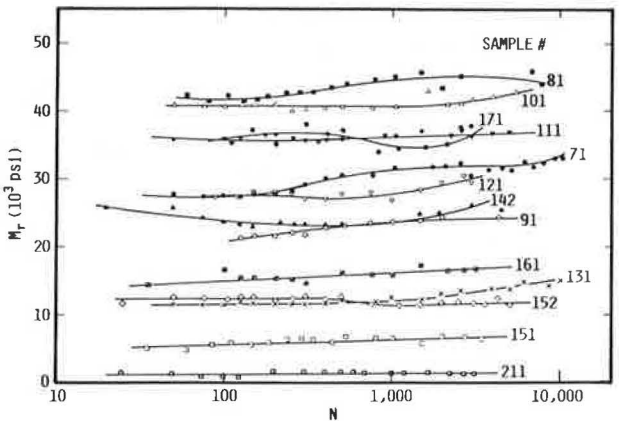

FIGURE 10 Resilient modulus versus number of load repetitions.

Table 3 gives the correlation array of the resilient modulus versus different variables. The modulus was most sensitive to changes in stress state. It increased with dynamic deviator stress as well as dynamic confining pressure. In some samples, however, the modulus decreased with increasing deviator stress for low values of deviator stress (less than 10 psi). At high stress levels, the modulus reached a stable maximum value. The measured results from Samples 82, 22, and 240 were compared to predictions from Equation 3 and verified this equation satisfactorily. However, only the results from Sample 82 for a stress level $(\sigma_1 - \sigma_3)$ above 10 psi agreed with Equation 3 (Figure 11). Table 5 gives the results of statistical analysis of the data.

A logarithmic relationship was observed between the constants k_1 and k_2 in Equation 3 (10). The

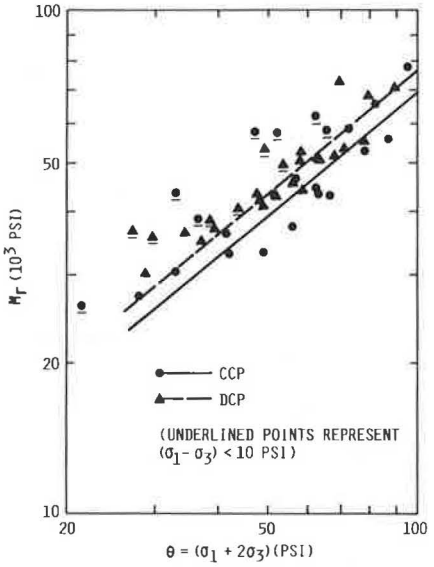

FIGURE 11 M_R versus θ for sample 82.

TABLE 5 Regression Results of Equation 2

Sample No.	Test Type	k_1	k_2	Correlation Coefficient
82[a]	CCP	1.704×10^3	0.802	0.949
	DCP	2.790×10^3	0.703	0.953
22	DCP	5.450×10^3	0.526	0.860
240	DCP	1.760×10^3	0.749	0.953

[a]Only points with $(\sigma_1 - \sigma_3) > 0$ were included.

data obtained by Allen (4) for DCP and CCP tests and by Hicks (5) for dry and wet samples are plotted in Figure 12. The linear relationship on the semilog plot between k_1 and k_2 is apparent in that figure. The relationship could be expressed as

$$k_2 = H_1 - H_2 \log k_1 \quad (13)$$

where H_1 and H_2 are regression constants. Values of H_1 and H_2 for the presented data are shown in Figure 12. It should be mentioned that Hicks' data presented in Figure 12 were for different materials, gradations, and fines contents. Apparently Equation 13 holds regardless of these factors. That is, H_1 and H_2 are dependent only on the type of testing (CCP or DCP).

A final comment should be made on the effect of static stresses on which dynamic stresses were superimposed. The static stresses were necessary to assure proper sample seating and conditioning in the vertical direction and to avoid negative confining pressure from occurring during the test. It was found that changing static confining pressure within 3 psi did not affect the resilient modulus significantly. On the other hand, the deviator static

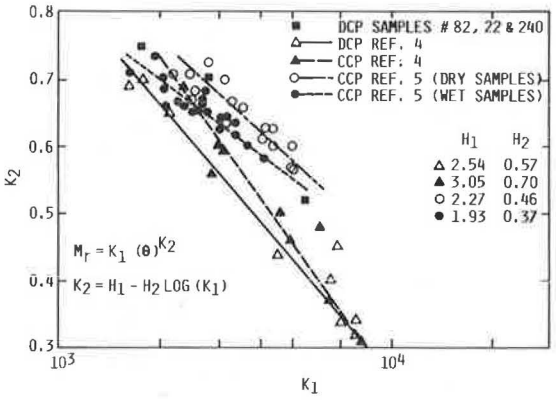

FIGURE 12 Interrelationship between k_1 and k_2.

stress had significant effect on the modulus (Figure 13). Doubling the value of the static deviator stress from 3 to 6 psi could increase the resilient modulus by 50 percent or more. In any standardization of the dynamic test procedure on granular material, this factor should be taken into account. That is, a standard seating static stress should be assigned in order to assure reproducible and comparable test results.

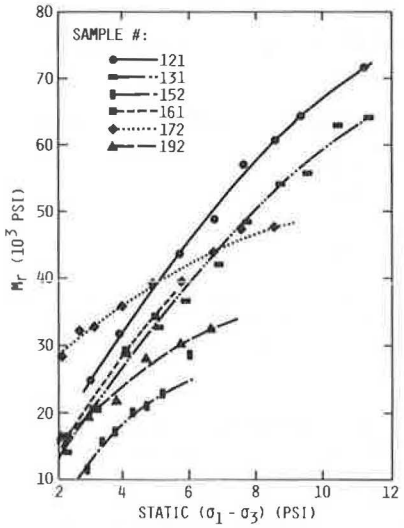

FIGURE 13 Resilient modulus versus static vertical stress.

SUMMARY AND CONCLUSIONS

A triaxial test program that applied time-variable confining pressure synchronized with deviator dynamic stress application was designed and performed on untreated granular base course material. Both residual and resilient characteristics were investigated during the program. Analyses of the results led to the following conclusions:

1. The rate of permanent strain accumulation decreases logarithmically with the number of load repetitions with excellent correlation. This is expressed in Equation 5.
2. Parameter m in Equation 5 was found to vary in the range of 0.7 to 0.9 for the material tested, with a mean value of 0.804.
3. Parameter A in Equation 5 was expressed in a power form as a function of octahedral stress ratio and resilient modulus, Equation 11.
4. The resilient modulus for granular material was found to be most sensitive to stress state. Equation 3 was verified in most of the test results.
5. Constants k_1 and k_2 in Equation 3 were intercorrelated through a logarithmic relationship, Equation 13.
6. The resilient modulus of granular material was found to be sensitive to seating static vertical stress. This should be considered when standardizing the dynamic testing process for granular material.
7. Further studies are needed to validate the applicability of these conclusions to other types and conditions of base course materials.

REFERENCES

1. The AASHO Road Test: Report 5--Pavement Research. HRB Special Report 61E. HRB, National Research Council, Washington, D.C., 1962.
2. H. Seed and C. Chan. Effect of Stress History and Frequency of Stress Application on Deformation of Clay Subgrades Under Repeated Loading. Proc., HRB, National Research Council, Washington, D.C., Vol. 37, 1958.
3. P. Pell and S. Brown. The Characteristics of Materials for the Design of Flexible Pavement Structures. Proc., Third International Conference on the Structural Design of Asphalt Pavements, London, England, 1972.
4. J. Allen. The Effect of Non-Constant Lateral Pressures of the Resilient Response of Granular Materials. Ph.D. dissertation. University of Illinois at Urbana-Champaign, 1973.
5. R. Hicks. Factors Influencing the Resilient Properties of Granular Materials. Ph.D. dissertation. University of California, Berkeley, 1970.
6. R. Barksdale. Laboratory Evaluation of Rutting in Base Course Materials. Proc., Third International Conference on Structural Design of Asphalt Pavements, London, England, 1972.
7. I. Kalcheff. Characteristics of Graded Aggregates as Related to Their Behavior Under Varying Loads and Environments. Presented at Conference on Graded Aggregate Base Material in Flexible Pavements, Oak Brook, Ill., 1976.
8. J. Rauhut, J. O'Quin, and W. Hudson. Sensitivity Analysis of FHWA Structural Model VESYS II, Vol. 1: Preparatory and Related Studies. Report FHWA-RD-76-23. FHWA, U.S. Department of Transportation, March 1976.
9. J. Morgan. The Response of Granular Materials to Repeated Loading. Proc., Third Conference of the Australian Road Research Board, 1966.
10. S. Khedr. Residual Characteristics of Untreated Granular Base Course and Subgrade Soils. Ph.D. dissertation. Ohio State University, University Park, 1979.
11. Y. Chou. Analysis of Permanent Deformations of Flexible Airport Pavements. Report FAA-RD 77-6. U.S. Army Engineer Waterways Experiment Station, Vicksburg, Miss.
12. S. Brown, B. Brodrick, and C. Bell. Permanent Deformation of Flexible Pavements. Research Report to ERO. U.S. Army, University of Nottingham, United Kingdom, 1977.

Publication of this paper sponsored by Committee on Strength and Deformation Characteristics of Pavement Sections.